

Determination of Fluoride in Drinking Water and Sea Water by Aluminium Monofluoride Molecular Absorption Spectrometry Using an Electrothermal Graphite Furnace

Milagros Gomez Gomez, Maria Antonia Palacios Corvillo and Carmen Cámara Rica

Departamento de Química Analítica, Facultad de Ciencias, Ciudad Universitaria, Universidad Complutense de Madrid, Madrid 2040, Spain

A method is presented for the determination of trace levels of fluoride in drinking water and sea water, based on the formation of aluminium monofluoride in an electrothermal graphite furnace, followed by molecular absorption at 227.45 nm. Two linear intervals extending over wide F^- concentration ranges (0–0.2 and 0.2–0.4 $\mu\text{g ml}^{-1}$ for the peak-height relationship and 0–1 and 1–2 $\mu\text{g ml}^{-1}$ for the peak-area relationship) were found.

The proposed method was applied to natural and artificial drinking and sea waters from a variety of sources and with different saline contents. The detection limit was 8 ng ml^{-1} and the determination limit 20 ng ml^{-1} . The peak-height precision at 0.2 and 0.4 $\mu\text{g ml}^{-1}$ of F^- was 5% and 7%, respectively.

F^- contents can be measured with a simple sample dilution. The use of a deuterium lamp allows simultaneous background correction. Interferences from cations, acidic media and anions were investigated.

Keywords: Aluminium fluoride molecular absorption spectrometry; electrothermal vaporisation; fluoride determination; drinking water analysis; sea water analysis

In recent years the determination of fluorine in complex biological samples has become increasingly important because of its clinical and environmental implications,^{1,2} and extensive research has been carried out in response to the demand for analytical methods.

Fluoride is commonly determined using ion-selective electrodes (ISEs).^{2,3} These are only sensitive to free fluoride ion, however, and losses from or contamination of samples may occur during the pre-treatment procedure to liberate F^- from complexes. The direct alizarin complexone spectrophotometric method^{4,5} and the Eriochrome cyanine method^{6,7} for fluoride are widely used, but some cations and anions seriously interfere and usually the separation of fluorine by distillation, ion exchange, microdiffusion, pyrohydrolysis, etc., is required.⁸ Methods based on enhancement or suppression of the atomic absorption signal of certain metals that interact with the halide have been reported,⁹ but they are normally insensitive and inconvenient for practical use.

The aluminium monofluoride molecular absorption (AlF MA) procedures described by Tsunoda *et al.*¹⁰ and Dittrich¹¹ were developed for the ultra-trace determination of fluoride. They are based on the formation of aluminium monofluoride in a graphite furnace and exploitation of a sharp molecular band near 227.45 nm. This method has considerable advantages: (i) small sample volume; (ii) fairly high sensitivity; and (iii) suitability for total fluorine determination with little or no sample pre-treatment (biological samples can be digested in the graphite furnace during the ashing step). However, a drawback of this method is the occurrence of significant interferences from matrix anions and cations.¹²

In this study we examined the analytical parameters and matrix-ion interferences that influence the efficiency of the diatomic AlF formation and the precision of the AlF MA method. The procedure developed provides the required accuracy and precision for the determination of the fluorine content of drinking water and sea water. The results for drinking waters have been compared with those obtained using fluoride ISEs.

Experimental

Apparatus

A Perkin-Elmer 1100B atomic absorption spectrometer equipped with a deuterium lamp for simultaneous background

correction was used for AlF MA measurements. A furnace programme (HGA 400) and pyrolytic graphite furnaces with either a L'vov platform or a laboratory-made platform (a flat platform with a 2 mm deep, 5 mm diameter depression) were used. A platinum hollow-cathode lamp was used as a light source for molecular absorption. The spectral band pass was 0.07 nm in all instances. Argon (flow-rate 200 ml min^{-1}) was used to purge air from the cuvette. A pH/mV meter (Crison Digit 501), a fluoride ISE (Orion Model 94-09) and a reference electrode (Ag - AgCl, Orion 90-01) were used in the potentiometric method.

Chemicals

All reagents were of analytical-reagent grade from Merck. A standard fluoride solution was prepared by dissolving Suprapur NaF in distilled water. All metal ions were in the form of nitrates. The buffer solution used for adjustment of the total ionic strength in the fluoride ISE method was TISAB III containing cyclohexane-1,2-diaminetetraacetic acid (Orion 940911). Aluminium nitrate solution (10⁻² M) was used.

Procedure

The experimental procedure for the determination of fluorine in drinking and sea water is summarised in Table 1. Drinking

Table 1. Experimental procedures for AlF molecular absorption with a graphite furnace

Procedure	Temperature/ °C	Ramp/s	Hold/s	Ar flow-rate/ ml min^{-1}
1.* Application of Al^{3+} solution (20 μl)	—	—	—	310
2. Drying	110	20	30	310
3. Stop and cooling of furnace	—	—	—	—
4. Application of F^- solution (10 μl)	—	—	—	—
5. Drying	110	20	30	310
6. Ashing I	700	10	30	310
7. Ashing II	700	0	2	0 (stop flow)
8. Vaporisation . .	2400	0	4	0 (stop flow)

* Aluminium nitrate solution and strontium nitrate concentrations 0.01 M.

water was added to the furnace after drying the aluminium solution. When sea waters were analysed, a dilution of greater than 1 + 20 with de-ionised water was necessary in order to avoid interference from the saline matrix. The standard additions method was applied for measurements.

Results and Discussion

Effect of Furnace Type and Temperature Programme on AlF Radical Formation

To study the effect of the graphite tube and shape, the proposed method was tested with (a) spectrally pure high-density graphite tubes, (b) pyrolytically coated graphite tubes, (c) a L'vov platform with a pyrolytically coated graphite tube and (d) a laboratory-made platform with a pyrolytically coated graphite tube. The results obtained are shown as relative absorbance in Table 2. Pyrolytically coated graphite tubes gave a 60% higher sensitivity than normal graphite tubes. The use of the L'vov and laboratory-made platforms provided longer furnace lifetimes, slightly better precision and greater sensitivity (100% higher) than normal graphite tubes.

Vaporisation temperatures higher than or equal to 2700 °C for 7 s for AlF formation have been used by different workers^{13,14} and ashing temperatures in the range 700–1000 °C have been recommended.¹³ To investigate whether such high temperatures are justified, several programmes with AlF vaporisation temperatures ranging from 2000 to 2800 °C and ashing temperatures from 700 to 1400 °C, were tested for a variety of hold times. The results are plotted in Fig. 1. In the ashing step a constant absorbance signal was obtained from 700 to 1000 °C. The decrease in signal above 1000 °C can be explained by losses of fluoride at high temperature. Vaporisa-

tion temperatures from 2400 to 2800 °C gave a constant signal. As suggested by Tsunoda *et al.*,¹⁰ 2400 °C corresponds to the maximum atomic absorption by Al. It therefore seems that atomisation of Al is an essential step in the formation of the AlF radical.

The effects of varying the ramps, hold times and argon flow-rates were studied using a 700 °C ashing temperature and a 2400 °C vaporisation temperature. No reason was found to justify the use of the long vaporisation hold times suggested in the literature. Hence a 4-s hold time and maximum heating were chosen for further experiments. Nevertheless, integration of peak areas gave negative values at fluoride concentrations lower than 0.2 p.p.m. This could be explained by background over-compensation as a result of the excessive integration time. As can be seen in Fig. 2, which gives background and analyte signals for a 0.2 µg ml⁻¹ fluoride concentration, the entire analyte peak appears before 1.5 s. Hence peak height calculated with a 1.5-s integration time provided similar absorbance values to those obtained using a 4-s integration time, and negligible negative peak areas in the absence of fluoride. This integration time therefore allows the use of both peak area and peak height in calculations based on the analytical signal.

The size and stream of the inert gas flow in the furnace significantly affect the production of diatomic molecules.¹⁴ Normal internal flow (310 ml min⁻¹) and miniflow (50–150 ml min⁻¹) were employed in the ashing and vaporisation steps, stop flow also being used in the latter. The use of an argon stop flow during the vaporisation step gave an analytical signal 60% greater than that with a miniflow and 100% greater than that with a normal flow. In the ashing step the AlF MA signal was independent of the argon flow used but the precision was improved from 5 to 3% by a second ashing step using a 2-s hold time and stop flow, before the vaporisation step.

Matrix Modifier

It is well established that a matrix modifier is necessary for generating the AlF radical and to increase the sensitivity of the determination of fluoride. Usually Sr²⁺ + Ni²⁺ or Sr²⁺ + Fe²⁺ are chosen. Sr²⁺ is used (i) to reduce the volatilisation of fluoride in the ashing and vaporisation steps, through an immobilisation effect, and (ii) to inhibit the strong thermal hydrolysis by Al³⁺ in the drying and ashing steps and maintain fluoride in the graphite furnace until the AlF formation temperature is reached.¹⁵ The role of Ni²⁺ or Fe²⁺ is to decrease the background.^{10,16} Dittrich and Meister¹⁷ reported that Ba²⁺ gave a more coincident evaporation of the barium halide species and aluminium.

The results given by the proposed method for some of the usual matrix modifier concentrations are displayed in Table 3. They show that 20 µl of 10⁻² M Sr²⁺ + 10⁻² M Al³⁺ solution enhances the F⁻ signal by 100% with respect to that obtained using only Al³⁺. The results are precise above 0.05 µg ml⁻¹ of F⁻. The presence of Ni²⁺ or Fe²⁺ in high concentrations

Table 2. Relative absorbance and relative standard deviation for AlF molecular absorption with different furnace materials (0.20 µg ml⁻¹ of fluoride). Five replicate analyses of each sample were carried out

Furnace	Relative absorbance	RSD, %
Normal graphite	1.0	5
Pyrolytically coated graphite	1.6	5
L'vov platform + pyrolytically coated graphite	2.0	4
Laboratory-made platform + pyrolytically coated graphite	2.0	4

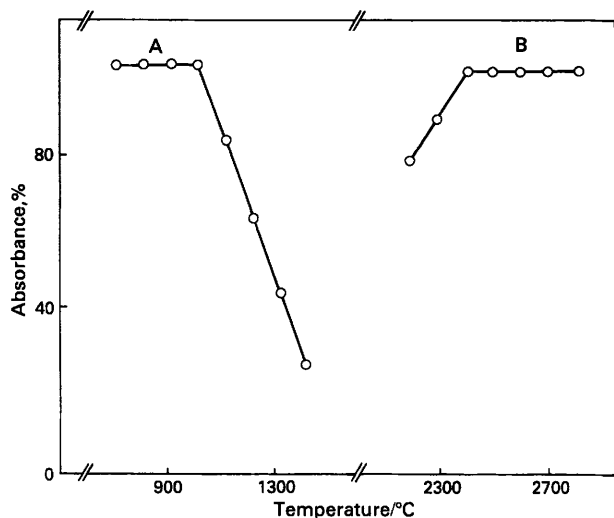


Fig. 1. Influence of furnace programme. (A) Effect of ashing temperature and (B) effect of vaporisation temperature on the AlF MA method (10 µl of 0.2 µg ml⁻¹ F⁻ + 20 µl each of 0.01 M Al and 0.01 M Sr solutions)

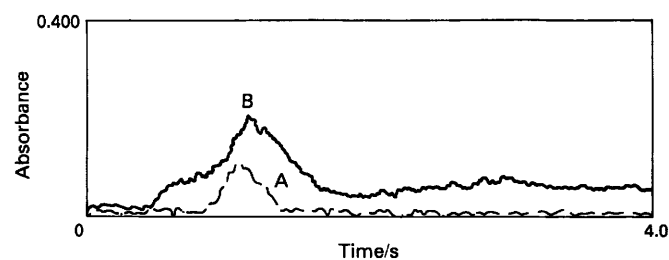


Fig. 2. Background and analyte signals; AlF MA method with an integration time of 4 s. (A) Analyte signal (10 µl of 0.2 µg ml⁻¹ F⁻ + 20 µl each of 0.01 M Al and 0.01 M Sr solutions) and (B) background signal

(10^{-2} M) diminishes the background and also the sensitivity. Ba^{2+} added as a matrix modifier in the form of $Ba(OH)_2$ or $Ba(NO_3)_2$ does not produce any increase in sensitivity compared with the use of Sr^{2+} . A high concentration (5×10^{-2} M) of Al^{3+} and Ba^{2+} as nitrate increases the sensitivity but also increases the background.

Different orders and volumes of reagent addition, from 25 to 5 μ l, were tested. The absorbance values for 1 ng of total fluoride were 0.060 ± 0.005 , 0.060 ± 0.002 , 0.055 ± 0.003 and 0.054 ± 0.004 for 5-, 10-, 20- and 25- μ l sample volumes, respectively. The best sensitivity and precision were given by a 10- μ l fluoride sample.

Calibration graphs were prepared using Sr^{2+} , Ba^{2+} and $Sr^{2+} + Ni^{2+}$ as matrix modifiers. The results are shown in Fig. 3. At low fluoride concentrations Ba^{2+} as nitrate shows advantages over Sr^{2+} , giving a linear calibration graph (Fig. 3, C) at F^- levels below 0.05 μ g ml $^{-1}$. In contrast, the use of Sr^{2+} at F^- concentrations lower than 0.05 μ g ml $^{-1}$ gives higher absorbances than expected. The same anomalous behaviour was found by Itai *et al.*,¹⁸ although they obtained a negative deviation.

Plots of peak height for the three matrix modifiers show two different linear intervals, from 0 to 0.2 and from 0.2 to 0.4 μ g ml $^{-1}$ of F^- . The slope of the second linear interval is half that of the first. This could be attributed to the formation of aluminium fluoride radicals with different stoichiometries. In the peak-area plots (Fig. 4), the two linear intervals extend over wider F^- concentration ranges (0–1 and 1–2 μ g ml $^{-1}$). It

is therefore advisable to utilise peak-height measurements at F^- concentrations lower than 0.2 p.p.m. and peak-area measurements at F^- concentrations above 0.2 p.p.m.

Interferences

The most common cations and anions present in sea-water and biological samples, and also various acidic media, were tested to determine their effect on AIF radical formation. The results, given in Table 4, indicate that cations do not

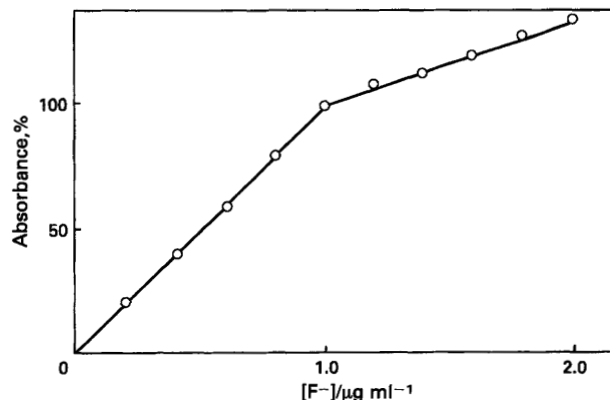


Fig. 4. Peak area calibration graph for fluoride in the presence of 20 μ l each of 0.01 M Al, 0.01 M Sr and 5×10^{-3} M Ni solutions

Table 3. Net relative absorbance obtained with different matrix modifiers. 10 μ l of a 0.1 μ g ml $^{-1}$ standard fluoride solution were applied. Five replicate analyses of each sample were carried out

Matrix modifier	Relative absorbance, %
10 μ l Al^{3+} (10^{-2} M)	100 ± 10.5
20 μ l Al^{3+} (10^{-2} M)	108 ± 10
10 μ l ($Al^{3+} + Sr^{2+}$, 10^{-2} M each)	189 ± 7
20 μ l ($Al^{3+} + Sr^{2+}$, 10^{-2} M each)	205 ± 7
20 μ l ($Al^{3+} + Sr^{2+} + Fe^{2+}$, 10^{-2} M each)	189 ± 8.5
20 μ l ($Al^{3+} + Sr^{2+}$, 10^{-2} M each, + Fe^{2+} , 5×10^{-3} M)	192 ± 8.5
20 μ l ($Al^{3+} + Sr^{2+}$, 10^{-2} M each, + Fe^{2+} , 5×10^{-2} M)	167 ± 8
20 μ l ($Al^{3+} + Sr^{2+} + Ni^{2+}$, 10^{-2} M each)	162 ± 6
20 μ l ($Al^{3+} + Sr^{2+}$, 10^{-2} M each, + Ni^{2+} , 5×10^{-3} M)	200 ± 5.5
20 μ l ($Al^{3+} + Sr^{2+}$, 10^{-2} M each, + Ni^{2+} , 5×10^{-2} M)	150 ± 6
20 μ l (Al^{3+} , 5×10^{-2} M, + Ba^{2+} , 5×10^{-2} M)*	240 ± 5
20 μ l (Al^{3+} , 10^{-2} M, + Ba^{2+} , 5×10^{-3} M)*	205 ± 5
20 μ l (Al^{3+} , 5×10^{-2} M, + Ba^{2+} , 5×10^{-2} M)†	154 ± 7
20 μ l (Al^{3+} , 10^{-2} M, + Ba^{2+} , 10^{-2} M)†	164 ± 5

* Barium solution as nitrate.

† Barium solution as hydroxide.

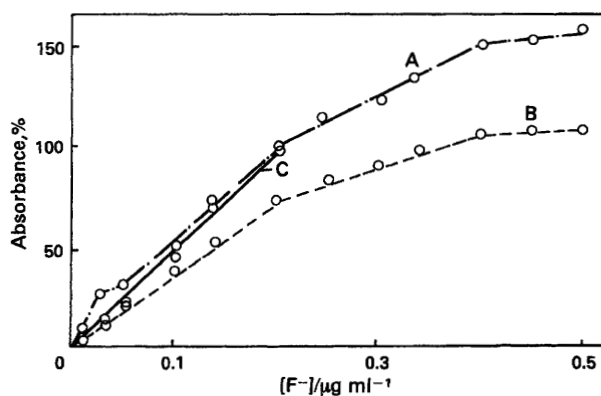


Fig. 3. Peak height calibration graphs for fluoride in the presence of (A) 20 μ l each of 0.01 M Al and 0.01 M Sr solutions; (B) 20 μ l each of 0.01 M Al, 0.01 M Sr and 5×10^{-3} M Ni solutions; and (C) 20 μ l each of 0.01 M Al and 5×10^{-3} M Ba solutions

Table 4. Interferences. The sample solution contained 0.2 μ g ml $^{-1}$ of F^- plus x μ g ml $^{-1}$ of interfering ion. Aluminium nitrate solution and strontium nitrate concentrations, 0.01 M. Cations were in the nitrate form unless stated otherwise

Element/compound	Concentration/ μ g ml $^{-1}$	Absorption, %
Ba^{2+}	1000	105
Ca^{2+}	30	100
	100	64
	1000	16
Cd^{2+}	500	100
	1000	80
Co^{2+}	500	100
	1000	75
Cr^{3+}	700	100
	1000	72
Cu^{2+}	500	100
	1000	67
Fe^{2+}	300	100
	1000	80
K^+	200	100
	1000	80
Mg^{2+}	100	100
	1000	79
Mn^{2+}	400	100
	1000	40
Na^+	200	100
	1000	80
NaOH	10^{-2} M	50
Ni^{2+}	1000	100
Pb^{2+}	500	100
	1000	90
Zn^{2+}	1000	100
H_2SO_4	10^{-2} M	35
	10^{-1} M	29
HCl	10^{-2} M	80
	10^{-1} M	30
Cl^- (as NaCl)	500	90
	1000	64
	4000	14
Br^- (as KBr)	1000	100
	2000	80
I^- (as KI)	2000	100

significantly increase the analytical signal when Sr^{2+} is added as a matrix modifier. The serious interference by Ca^{2+} may be attributed to a plasma effect. Sodium interferes more seriously when added as NaOH than as NaNO_3 . As regards acidic media, the signal decreases with increasing acid concentration, probably owing to the release of volatile HF by pyrohydrolysis reactions.

Halide ions interfere in the order $\text{Cl}^- > \text{Br}^- > \text{I}^-$. As the purpose of this work was the determination of fluoride in drinking and sea water, the samples are diluted for analysis, resulting in final concentrations of Cl^- , Br^- and I^- that are below the interference levels.

Determination of Fluorine in Fresh Water and Sea Water

The proposed method was applied to natural and artificial drinking and sea waters from a variety of sources and with different saline contents. The analytical conditions were those indicated in the procedure. The detection limit was 8 ng ml^{-1} and the determination limit 20 ng ml^{-1} . The peak-height precision at 0.2 and $0.4 \text{ } \mu\text{g ml}^{-1}$ of F^- was 5% and 7%, respectively. The results are shown in Table 5.

To verify the accuracy of the method, artificial drinking water containing 5 mM NaCl , $5 \text{ mM Na}_2\text{SO}_4$, $2.5 \text{ mM Ca}(\text{HCO}_3)_2$ and $0.7 \text{ } \mu\text{g ml}^{-1}$ of F^- as NaF and artificial sea water containing 0.5 M NaCl , 0.8 mM KBr , 4 mM NaHCO_3 and $1.5 \text{ } \mu\text{g ml}^{-1}$ of F^- as NaF were prepared. It was found that a 0–5-fold dilution of drinking water allowed the direct determination of fluorine without the need to counteract interferences due to matrix constituents. Standard additions were necessary in natural high-saline drinking waters (Barcelona and Badajoz), but in soft water no matrix effect was noted and analysis was possible using a calibration graph. The results were in good agreement with those obtained using a fluoride ion-selective electrode and with the fluorine content specified on the labels for mineral waters. When sea water was analysed, a dilution of greater than 1 + 20 was necessary in order to lower the Cl^- content below the interference level. Generally the F^- content of sea water is high enough to make this dilution possible. The results for artificial sea water were in good agreement with the known amount of F^- added. Finally, the analyses showed different F^- contents depending on the sea or ocean sampled.

Conclusions

An AIF MA method for determining the fluorine content of different kinds of water has been developed. The only sample treatment necessary is dilution. The use of a L'vov platform with a pyrolytically coated graphite tube and $\text{Sr}^{2+} + \text{Ni}^{2+}$ as matrix modifiers significantly improves the precision of the method. Two linear intervals extending over wide F^- concentration ranges ($0\text{--}0.2$ and $0.2\text{--}0.4 \text{ } \mu\text{g ml}^{-1}$ for the peak-height relationship and $0\text{--}1$ and $1\text{--}2 \text{ } \mu\text{g ml}^{-1}$ for the peak-area relationship) were found. A vaporisation temperature of 2400°C , a 4-s hold time and a 1.5-s integration time provided the best results.

The authors thank M. C. Moreno and I. Gomez del Rio for their collaboration and Max Gormann for revision of the manuscript. CAICYT (Project 85/0035) and the International Atomic Energy Agency are thanked for financial support.

Table 5. Determination of fluoride in drinking and sea waters. Five replicate analyses of each sample were carried out

Type of water	Sample origin*	Fluoride concentration/ $\mu\text{g ml}^{-1}$	
		Fluoride ISE	AIFMA
Drinking water	Artificial†	0.68 ± 0.04	0.70 ± 0.04
	Madrid 1	0.18 ± 0.03	0.18 ± 0.03
	Madrid 2	0.10 ± 0.03	0.09 ± 0.01
	Valencia	0.10 ± 0.03	0.10 ± 0.02
	La Coruña	0.05 ± 0.01	0.04 ± 0.02
	Barcelona	0.28 ± 0.03	0.27 ± 0.02
	Asturias 1	—	0.04 ± 0.01
	Asturias 2	—	0.08 ± 0.01
	Ribes mineral	0.16 ± 0.02	0.16 ± 0.02
	Font del Pi mineral	1.10 ± 0.05	1.15 ± 0.05
Sea water	Artificial‡	—	1.50 ± 0.05
	Cantabrian (Sangenjo)	—	1.70 ± 0.04
	Mediterranean (Barcelona)	—	1.45 ± 0.03
	Mediterranean (Oliva)	—	2.50 ± 0.05
	Atlantic (Huelva)	—	1.30 ± 0.03

* Madrid 1 from Lozoya Canal; Madrid 2 from the Santillana Canal; Asturias 1 from a village piped-water supply; Asturias 2 is bottled mineral water; Font del Pi mineral water states 1 p.p.m. of F^- on the label.

† Artificial drinking water, $0.70 \text{ } \mu\text{g ml}^{-1}$ of F^- added.

‡ Artificial sea water, $1.50 \text{ } \mu\text{g ml}^{-1}$ of F^- added.

References

- Cox, F. H., and Backer, O., *Caries Res.*, 1968, **2**, 69.
- Venkateswarlu, P., *Clin. Chim. Acta*, 1975, **59**, 277.
- Venkateswarlu, P., *Anal. Biochem.*, 1975, **68**, 512.
- Venkateswarlu, P., and Sita, P., *Anal. Chem.*, 1971, **43**, 758.
- Greenhalgh, R., and Riley, J. P., *Anal. Chim. Acta*, 1961, **25**, 179.
- Dixon, E. J., *Analyst*, 1970, **95**, 272.
- Dixon, E. J., Grisley, L. M., and Sawyer, R., *Analyst*, 1970, **95**, 945.
- Marzenko, Z., "Spectrophotometric Determination of Elements," Ellis Horwood, Chichester, 1976.
- García-Vargas, M., Milla, M., and Pérez-Bustamante, J. A., *Analyst*, 1983, **108**, 1417.
- Tsunoda, K., Fujiwara, K., and Fuwa, K., *Anal. Chem.*, 1977, **49**, 2035.
- Dittrich, K., "Analytische Anwendung der Spektroskopie Zweiatomiger Moleküle," paper presented at Analytikreffen (1978), Atomspektroskopie, Fortschritte und Analytische Anwendungen, Finsterbergen, GDR, December 1978.
- Dittrich, K., Shkinev, V. M., and Spivakov, B. V., *Talanta*, 1985, **32**, 1019.
- Venkateswarlu, P., Winter, L. D., Prokop, R. A., and Hagen, D. F., *Anal. Chem.*, 1983, **55**, 2232.
- Tsunoda, K., Chiba, K., Haraguchi, H., and Fuwa, K., *Anal. Chem.*, 1979, **51**, 2059.
- Dittrich, K., Vorgerg, B., Funk, J., and Beyer, V., *Spectrochim. Acta, Part B*, 1984, **39**, 349.
- Chiba, K., Tsunoda, K., Haraguchi, H., and Fuwa, K., *Anal. Chem.*, 1980, **52**, 1582.
- Dittrich, K., and Meister, P., *Anal. Chim. Acta*, 1980, **121**, 205.
- Itai, K., Tsunoda, K., and Ikeda, M., *Anal. Chim. Acta*, 1985, **171**, 293.

Paper 8/00436F

Received February 8th, 1988

Accepted March 24th, 1988